

SINDO1 Study of the Photoreaction of Tetramethylene Sulfoxide

Karl Jug,* Frank Neumann, and Hans-Peter Schluff

Theoretische Chemie, Universität Hannover, Am Kleinen Felde 30, 30167 Hannover, Germany

Received July 20, 1993*

The mechanism of the photochemical decomposition of tetramethylene sulfoxide (TMSO) was investigated by the semiempirical MO method SINDO1. The relevant singlet and low-lying triplet potential energy hypersurfaces were studied with limited configuration interaction (CI). It was found that the main reaction products ethene, cyclobutane, cyclopropane, propene, and 1-butene are formed by concerted multiple bond fragmentations. These results differ from previous assumptions that α -cleavage is the main reaction channel. The energy data are supplemented by valence classification of diradical structures.

1. Introduction

The study of photochemical reaction mechanisms of heterocyclic compounds is an important topic for the understanding of formation and decomposition of ring systems. These can be classified as conjugated or saturated systems. For heterocyclic aromatic systems rearrangements are the major channel, and the processes are characterized by a permutation of ring atoms. Different mechanisms have been proposed for heterocycles containing nitrogen, oxygen, and sulfur.¹ We have studied such rearrangements for unsubstituted and substituted furan,² pyrrole,³ and thiophene⁴ by quantum chemical methods. For saturated ring systems decomposition is an important reaction pathway. Experimental work was extensively reviewed by Braslavsky and Heicklen.⁵ Among these systems compounds with sulfur are of particular interest because sulfur can be divalent, tetravalent, or hexavalent. The five-membered ring tetramethylene sulfide (TMS), tetramethylene sulfoxide (TMSO), and tetramethylene sulfone (TMSO₂) are representative of such a series. Comparative experimental studies of saturated ring systems with sulfur were published by several groups,⁶⁻⁹ and a mechanism was deduced.

The key questions are how the various products are formed and why certain products show a significant abundance in the formation process. The simplest explanation to the first question is an analysis of the various bond-breaking processes and subsequent reactions, with an understanding that the products are formed by the different ways of fragmentation of rings at different sites. The second question is more difficult to answer. The particular abundance of ethene in the photoreaction of the above five-membered ring systems prompted us to start a thorough theoretical investigation. Our first report on TMS¹⁰ resulted in a rather complex mechanism which could explain the relative yields of the observed hydro-

carbon products. In the present study we extend our investigations to TMSO to see the similarities of mechanism with other compounds. This includes TMS and cyclopentanone. The comparison of the latter compound with TMSO is warranted because both carbon and sulfur are tetravalent and have similar electronegativity.

2. Method of Calculation

The calculations were performed with the semiempirical MO method SINDO1¹¹ with an extension to second-row elements.¹² Since d orbital participation in the bonding of hypervalent compounds is a debated issue in both structural and mechanistic studies, we have included d sulfur orbitals. The accuracy of geometries and binding energies was documented in test calculations for a large number of sulfur compounds.¹³ The suitability of SINDO1 for photochemical reaction studies was demonstrated repeatedly; in particular, calculations on thiophene,⁴ tetramethylene sulfide,¹⁰ and cyclopentanone¹⁴ are relevant for the present study. In the following text, we denote the ground state by R₀, the vertically excited singlet states by R₁, R₂, etc., and the triplet states by ³R₁, ³R₂, etc. Intermediates on the lowest triplet surface are denoted by ³I_{1c}, ³I_{1d}, ³I_{1c}, ³I_{1e}, diradicals by ^{1,3}D, and intermediates on the first excited singlet state by I_{1e}. Minima including intermediates are characterized by exclusively positive roots of the force constant matrix, whereas transition structures have one negative root. Ground and excited equilibrium structures were optimized by a Broyden-Fletcher-Goldfarb-Shanno (BFGS) procedure¹⁵ as it was implemented by Zerner et al.¹⁶ Transition structures were located by geometry optimization with a Newton-Raphson procedure.¹⁷ Bond lengths were optimized within 1% and bond angles and dihedral angles within 1°. Excited state

* Abstract published in *Advance ACS Abstracts*, October 1, 1993.

(1) Pawda, A. In *Rearrangements in ground and excited states*; de Mayo, P., Ed.; Academic Press: New York, 1980; Vol. 3, p 501ff.
 (2) Buss, S.; Jug, K. *J. Am. Chem. Soc.* 1987, 109, 1044.
 (3) Behrens, S.; Jug, K. *J. Org. Chem.* 1990, 55, 2288.
 (4) Jug, K.; Schluff, H.-P. *J. Org. Chem.* 1991, 56, 129.
 (5) Braslavsky, S.; Heicklen, J. *Chem. Rev.* 1978, 77, 473.
 (6) Scala, A. A.; Colon, I. *Dep. Energy ITIC* 1978, 15, 11399.
 (7) Scala, A. A.; Colon, I.; Rourke, I. *J. Phys. Chem.* 1981, 85, 3603.
 (8) Dorer, F. H.; Salomon, K. E. *J. Phys. Chem.* 1980, 84, 1902.
 (9) Schuchmann, H. P.; von Sonntag, C. *J. Photochem.* 1983, 22, 55.

(10) Jug, K.; Neumann, F. In *Theoretical Chemistry: Linking Theory with Experiment*; Montero, L.; Smeyers, Y. G., Eds.; Kluwer: Dordrecht, 1992; pp 99ff.

(11) Nanda, D. N.; Jug, K. *Theor. Chim. Acta* 1980, 57, 95.
 (12) Jug, K.; Iffert, R.; Schulz, J. *Int. J. Quantum. Chem.* 1987, 32, 263.
 (13) Jug, K.; Iffert, R. *J. Comput. Chem.* 1987, 8, 1004.
 (14) Müller-Remmers, P. L.; Mishra, P. C.; Jug, K. *J. Am. Chem. Soc.* 1984, 106, 2538.
 (15) Fletcher, R. *Practical Methods of optimization*, 2nd ed.; J. Wiley & Sons: Chichester, 1987; p 57ff.
 (16) Head, J. D.; Weiner, B.; Zerner, M. C. *Int. J. Quantum Chem.* 1988, 33, 177.
 (17) Jug, K.; Hahn, G. *J. Comput. Chem.* 1983, 4, 410.

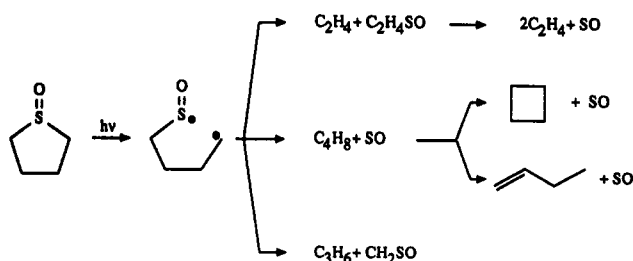


Figure 1. Reaction mechanism proposed from experiment.

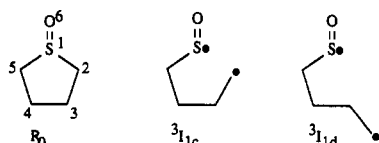


Figure 2. Structures of reactant R and intermediates I.

Table I. Bond Lengths r (Å), Bond Angles α , and Dihedral Angles ϕ (deg) of Reactant R and Intermediates I

state	R ₀ (C _s)	³ I _{1c}	³ I _{1d}
r_{12}	1.872	3.202	4.730
r_{15}	1.872	1.824	1.822
r_{16}	1.496	1.483	1.482
r_{23}	1.556	1.492	1.499
r_{34}	1.575	1.571	1.552
r_{45}	1.556	1.558	1.564
α_{123}	111.4	80.1	1.6
α_{154}	111.4	114.3	119.5
α_{516}	112.7	112.2	111.8
α_{216}	112.7	128.6	168.2
α_{234}	111.8	119.4	115.7
α_{345}	111.8	118.4	119.4
ϕ_{1234}	0.0	-39.5	-100.1
ϕ_{2345}	0.0	-19.9	178.6
ϕ_{1543}	0.0	46.4	2.1
ϕ_{4516}	116.5	124.5	178.0
ϕ_{3216}	-116.5	-153.4	85.5
ϕ_{3251}	0.0	118.9	-4.2

structures were optimized on their respective configuration interaction (CI) surfaces. Further details of the optimization procedure can be found in the furan treatment.² The size of configuration interaction was adjusted to guarantee an unambiguous qualitative explanation of the mechanism.

3. Results and Discussion

3.1 Structures. In order to understand the reaction mechanism of the photoreaction of TMSO, Figure 1 presents the reaction scheme which results from the experimental product distribution.^{7,8} This simplified scheme can be used as a starting point for the search of relevant structures on the ground- and excited-state potential hypersurfaces. The question is which intermediates and transition structures are involved in the pathways leading to the different products. From the scheme in Figure 1 also the relevance of diradical states in the reaction can be investigated. Since our studies of TMS¹⁰ and cyclopentanone¹⁴ have resulted in a variety of relevant structures, we have also taken these results into account in our search on TMSO. Figure 2 contains the relevant structures for the rearrangement and fragmentation processes in the photoreaction of this compound. Again cis (³I_{1c}) and trans (³I_{1d}) diradical structures were found as intermediates on the lowest triplet surface. Here,

Table II. Calculated Excitation Energies (eV) and Oscillator Strengths for TMSO

state	excitation energy	oscillator strengths
R ₁ (A'')	5.30	6.1×10^{-2}
R ₂ (A')	5.38	3.1×10^{-3}
R ₃ (A')	5.80	3.0×10^{-3}
R ₄ (A'')	6.24	9.2×10^{-3}
R ₅ (A'')	6.80	1.6×10^{-1}
R ₆ (A')	7.67	2.0×10^{-2}
R ₇ (A'')	8.56	1.4×10^{-2}

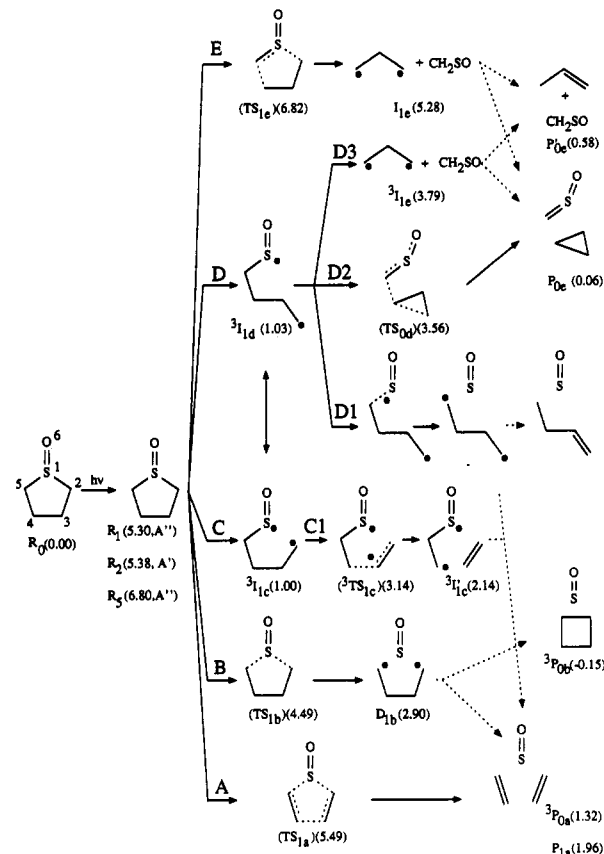


Figure 3. Reaction scheme.

one ring bond is broken, leading to an asymmetrical structure. The cis and trans structure allow further fragmentation. All these structures were already considered in cyclopentanone and TMS. The geometries of these structures are listed in Table I.

For the reactant R₀ the SO group is bent substantially out of the ring plane in C_s symmetry, but the force constant for distortion to the planar arrangement is small. To classify the structures ³I_{1c} and ³I_{1d} as diradicals, we have applied the valence reduction criterion¹⁸ in its valence partitioning form.¹⁹ On radical centers, where not all possible bonds are formed, the actual valence numbers are reduced by one unit compared with the normal valence numbers.²⁰ A diradical is a species with a valence reduction of about 2 for the whole molecule due to configuration interaction. For ³I_{1c} and ³I_{1d} we obtained 2.00, which is the sum of contributions from all atoms. The contributions of the ring atoms are as follows: ³I_{1c}, S₍₁₎ (0.53), C₍₂₎ (0.89), C₍₃₎ (0.01), C₍₄₎ (0.01), C₍₅₎ (0.00), O₍₆₎ (0.44); ³I_{1d}, S₍₁₎ (0.52), C₍₂₎ (0.88), C₍₃₎ (0.01), C₍₄₎ (0.07), C₍₅₎ (0.01), O₍₆₎ (0.44).

(18) Jug, K. *Tetrahedron Lett.* 1985, 26, 1437.(19) Jug, K.; Poredda, A. *Chem. Phys. Lett.* 1990, 171, 394.(20) Gopinathan, M. S.; Jug, K. *Theor. Chim. Acta* 1983, 63, 497, 511.

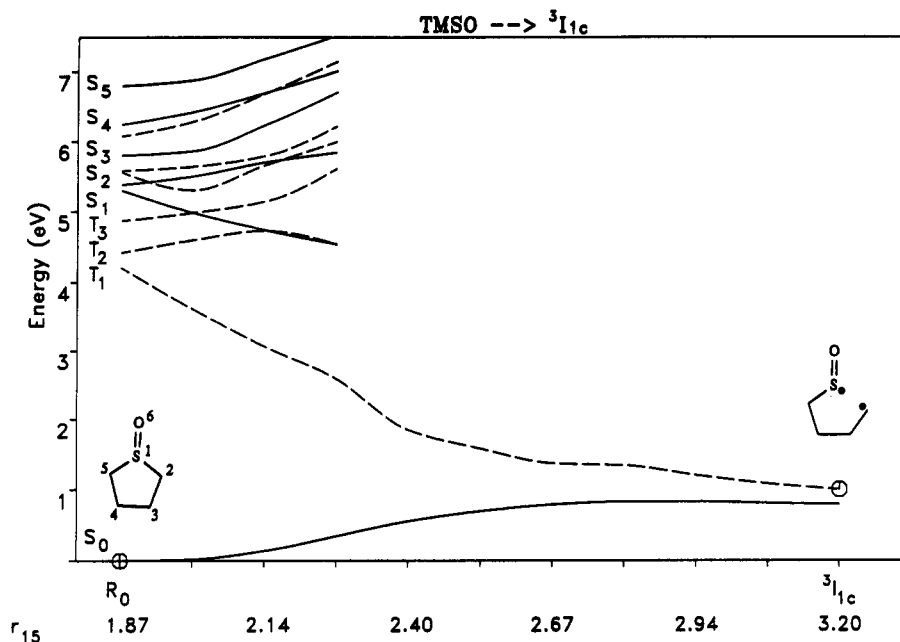


Figure 4. Potential curves for formation of diradical intermediate ${}^3I_{1c}$ (C); points of optimized geometry in circles.

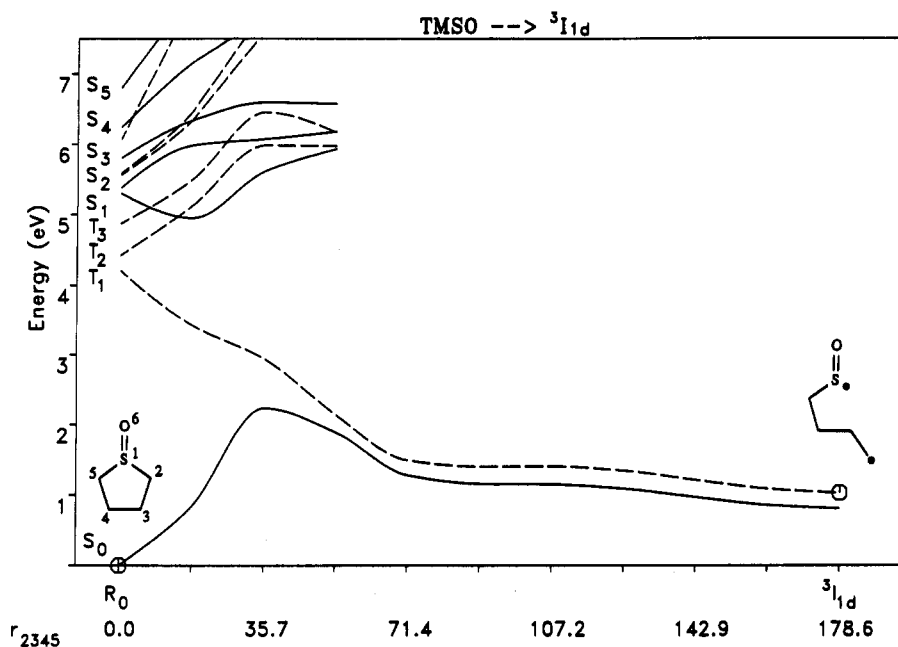


Figure 5. Potential curves for formation of diradical intermediate ${}^3I_{1d}$ (D); points of optimized geometry in circles.

This means that in both cases $C_{(2)}$ is a radical center and that the other radical contribution is delocalized in the SO group.

3.2 Vertical Excitations. From the experiments reported in the literature^{7,8} ethene was the main product accompanied by cyclopropane, propene, cyclobutane, 1-butene, butadiene, acetylene, and ethane. The relative abundance of one particular product in the product mixture depends on the excitation energy. Scala and co-workers irradiated TMSO with UV light of 147 nm which is equivalent to 8.44 eV and investigated the fragments by gas chromatography and mass spectrometry. Analysis of the product mixture resulted in 67% ethene, 10% propene, 7.5% acetylene, 7% 1-butene, 5% ethane, 2% cyclobutane, and 1% cyclopropane in the gas phase. Dorer and Salomon used a deuterium lamp (202–225 nm, 6.1–5.5 eV) and Zn (214 nm, 5.8 eV) and Cd (228 nm, 5.4 eV) lamps as light

sources. Again, ethene was by far the most abundant product. At low pressures and short wavelengths the C_3 product yield increased substantially and was more than two-thirds of the ethene yield with the cyclopropane yield always much lower than the propene yield. From the C_4 products only cyclobutane was found with the highest excitation energy, whereas for the lower excitation energies its occurrence was reduced in favor of 1-butene. We calculated the excitation energies with SINDO1^{11,12} under inclusion of CI. The 187×187 CI included single excitations from the six highest OMOs to the 14 lowest UMOs plus all double excitation from next HOMO and HOMO to LUMO and next LUMO. The selection was done in such a way that all close-lying HOMOs beyond the second were included in the calculation until the first large gap of 1.5 eV from HOMO6 to HOMO7 appeared in the sequence. This covers all relevant experimental

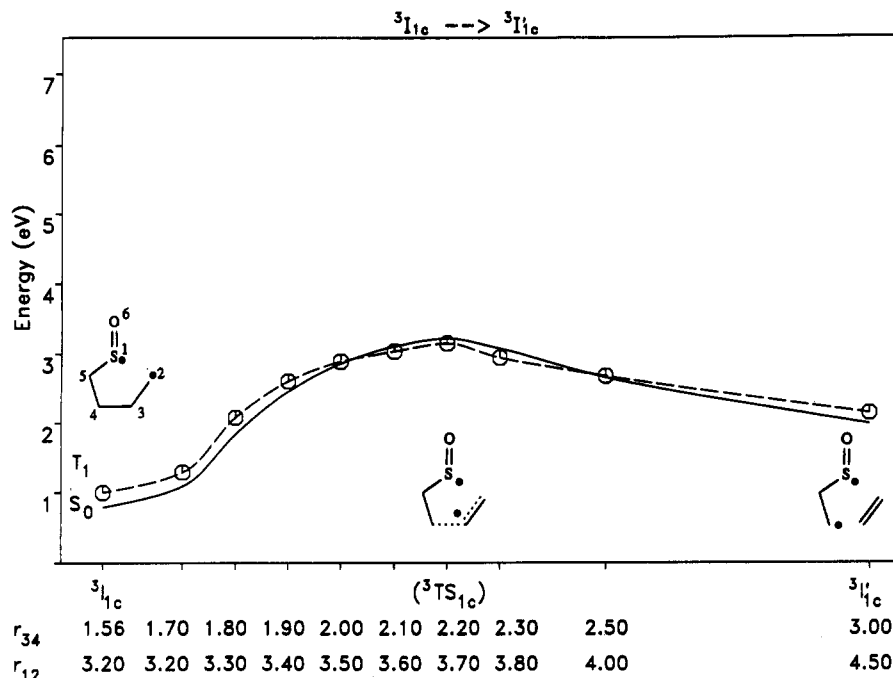


Figure 6. Potential curves for formation of ethene via ${}^3I_{1c}$ (C_1); points of optimized geometry in circles.

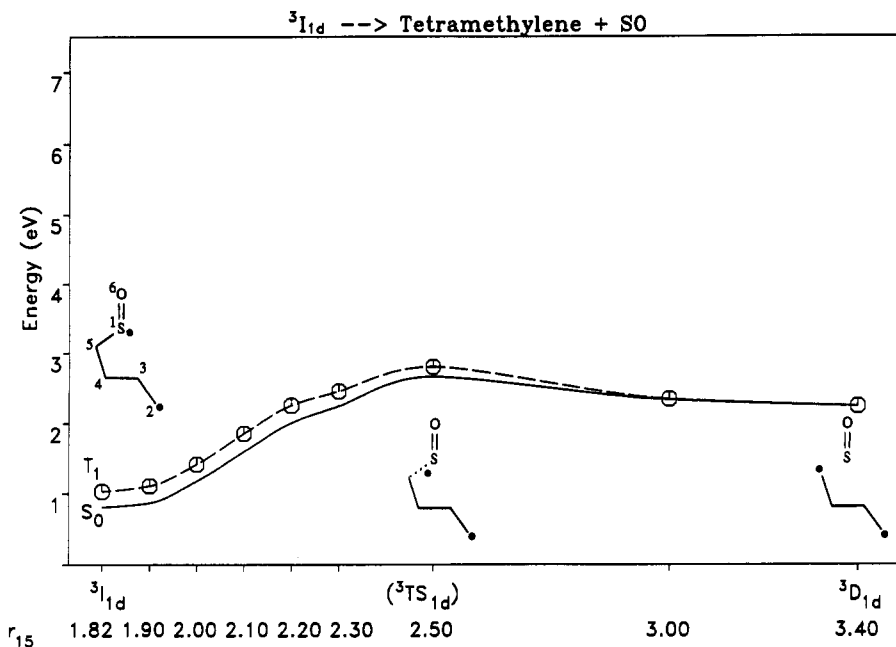


Figure 7. Potential curves for formation of tetramethylene via ${}^3I_{1d}$ (D_1); points of optimized geometry in circles.

excitation energies. Alternatively, one can define a maximum number of MOs between occupied and unoccupied MO levels involved in the single excitation procedure.²¹ Increase of the CI slightly lowered the excitation energies, but no significant change in the composition of the lowest relevant states occurred. Therefore, we could restrict ourselves to the 187×187 CI as a reference in the calculation of reaction pathways. From Table II it is apparent that the lowest excitation is to R_1 and the higher excitations to R_5 . This could be the explanation for the slight differences in the experimental results depending on the wavelength. But one could also argue that there

is fast relaxation in the Franck-Condon zone and only R_1 is populated outside of it.²²

3.3. Reaction Channels. After vertical excitation of TMSO there are four different reaction patterns possible: (A) concerted bond breaking of three ring bonds, (B) bond breaking of the two C-S bonds by an initially concerted ring bond opening, (C) and (D) bond breaking of a single ring bond and formation of diradical intermediates, and (E) simultaneous α - and β -cleavage. Taking into account most of the products found by the experimentalists and enlarging that set of intermediates, transition structures and products to account for this variety, we obtained the

(21) Reinsch, M.; Höweler, U.; Klessinger, M. *THEOCHEM* 1988, 167, 301.

(22) Michl, J. In *Excited States in Quantum Chemistry*; Nicolaides, C. A., Beck, D. R., Eds.; NATO ASI Series C 49; Reidel: Dordrecht, 1979; p 417ff.

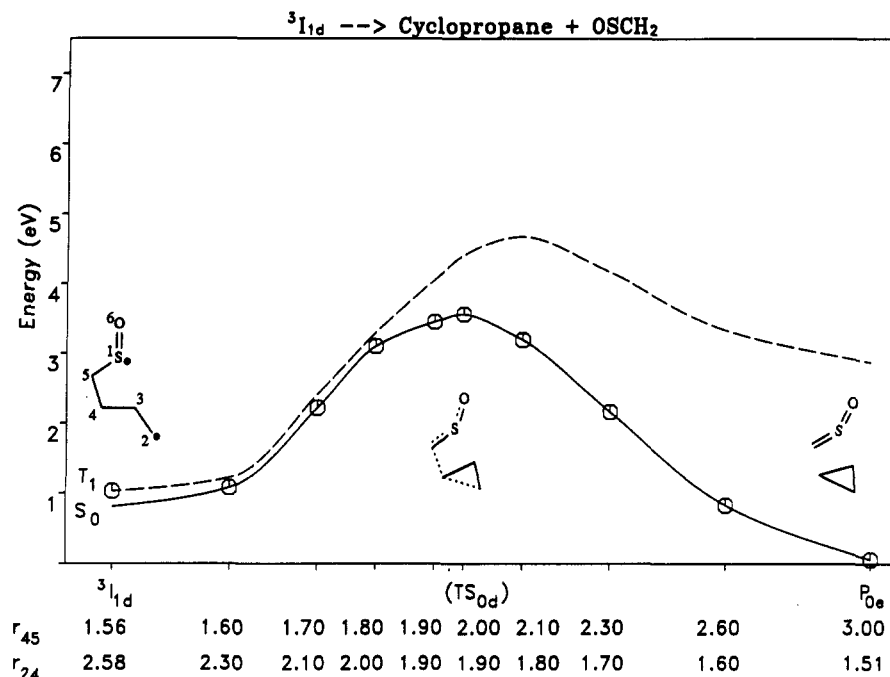


Figure 8. Potential curves for formation of cyclopropane via $^3I_{1d}$ (D_2); points of optimized geometry in circles.

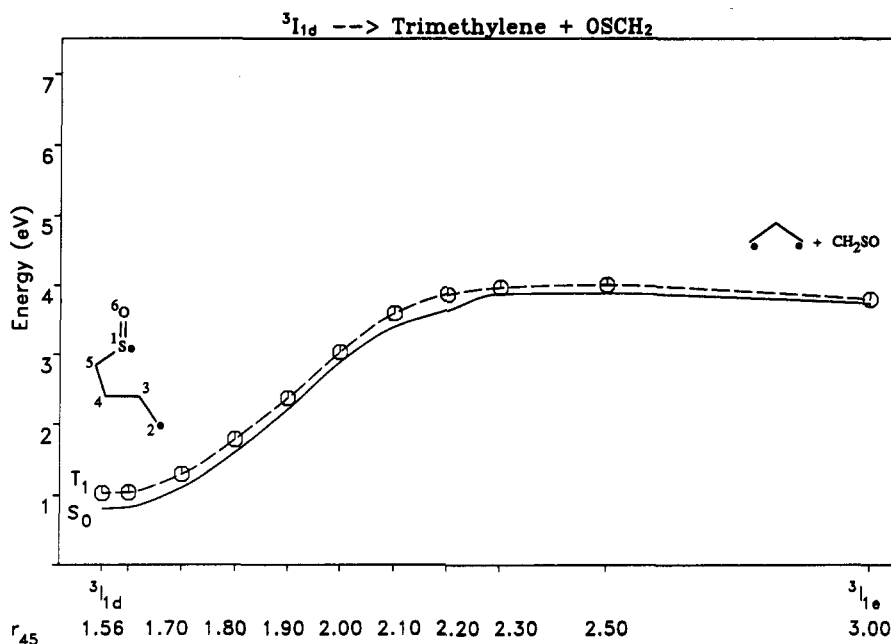


Figure 9. Potential curves for formation of trimethylene via $^3I_{1d}$ (D_3); points of optimized geometry in circles.

reaction scheme given in Figure 3. There are five kinds of products which were investigated: ethene, cyclobutane, 1-butene, cyclopropane, and propene. To decide which product is most likely to be found, it is necessary to investigate the kinetic control of product formation in addition to the thermodynamic control.

We therefore present reaction profiles for the 187×187 CI along relevant pathways for the most important products. Figures 4 and 5 contain potential curves of the ground and triplet states for the formation of the diradical intermediates $^3I_{1c}$ and $^3I_{1d}$ which could be the initial step in the formation of several products. All points between the fully optimized geometries of R_0 and the intermediates $^3I_{1c}$ and $^3I_{1d}$ are linearly interpolated. After initial excitation the first excited singlet in the Franck-Condon zone is reached either directly or after fast internal

conversion (IC) from higher lying singlet states. After intersystem crossing (ISC) and again IC, the lowest triplet state is reached. This state relaxes to either $^3I_{1c}$ or $^3I_{1d}$ since there are no barriers for these reactions. From $^3I_{1c}$ the reaction process branches to $^3I'_{1c}$. From $^3I_{1d}$ tetramethylene, cyclopropane, and trimethylene could be formed. Both pathways can formally lead to ethene formation. We discuss the pathway to $^3I'_{1c}$ first, since it involves an immediate formation of one ethene molecule. The potential curves for pathway C_1 are presented in Figure 6. There are two fully optimized structures $^3I_{1c}$, $^3I'_{1c}$ and interpolation along the new reaction coordinate r_{34} for breaking of the second ring bond. The bond length r_{34} was set constant whereas all other coordinates along the pathway were optimized. There is singlet-triplet degeneracy between S_0 and T_1 at the geometry of $^3I'_{1c}$. From

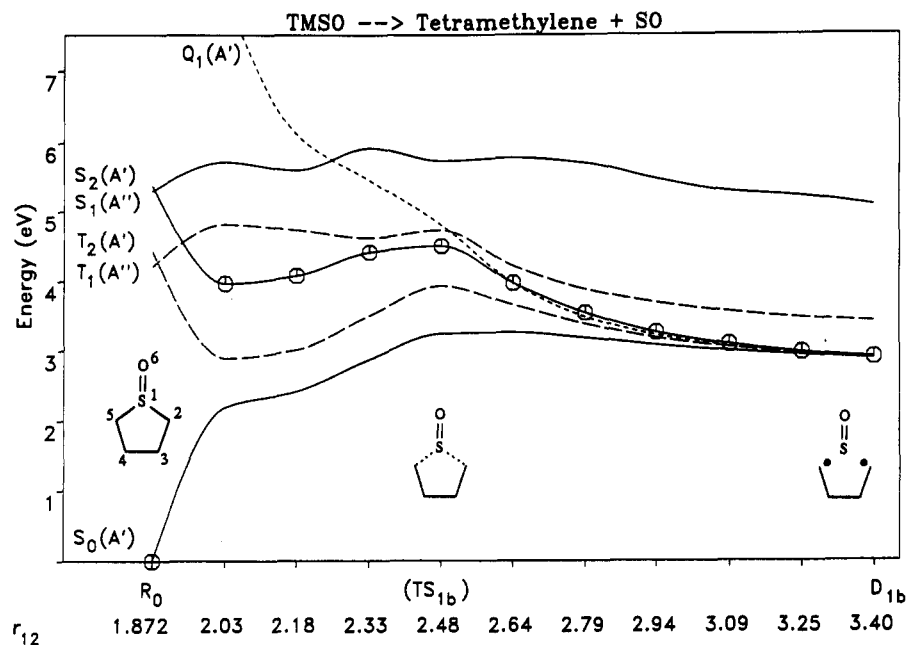


Figure 10. Potential curves for formation of tetramethylene and excited SO via R_2 (A'') (B); points of optimized geometry in circles.

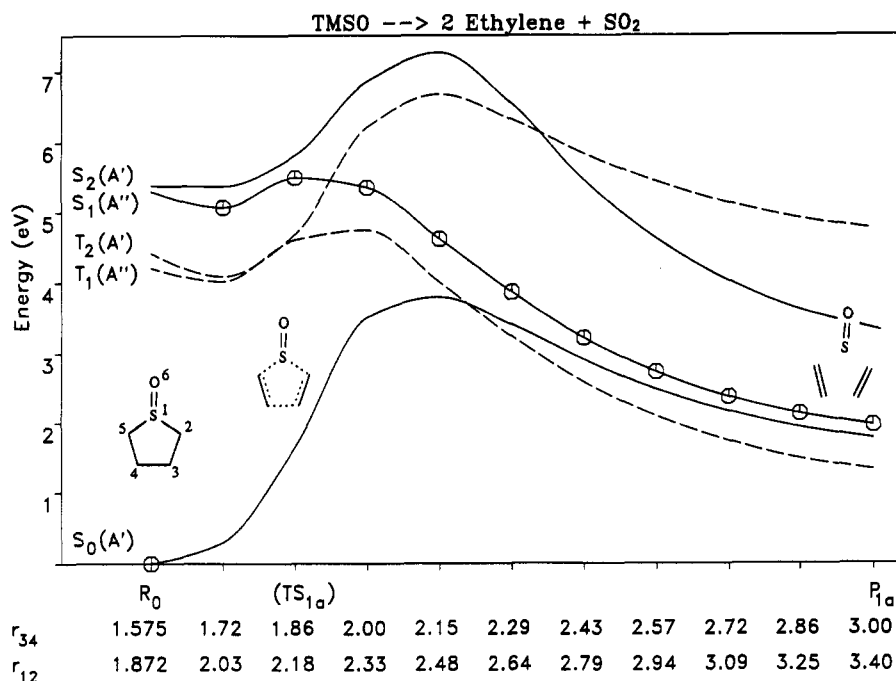


Figure 11. Potential curves for formation of ethene and excited SO via R_1 (A') (A); points of optimized geometry in circles.

$^3I_{1c}$, the system could proceed toward further dissociation to another ethene and the triplet ground state of SO. However, it is apparent from Figure 6 that the system is more likely to cross over to S_0 along this pathway, since T_1 is very close to S_0 in the initial step. This would lead to closure of the three-membered ring ethylene sulfoxide. Considering either the barrier of the reaction and the energy of $^3I_{1c}$, the ethene formation via $^3I_{1c}$ seems most unlikely because of thermodynamic and kinetic properties of pathway C_1 . Conversion of $^3I_{1c}$ to $^3I_{1d}$ is easily feasible because of the twixtyl character²³ of the diradical intermediates with a flat potential curve for rotation about the r_{34} bond. Tetramethylene is formed as a degenerate

diradical $^3D_{1d}$, which can in turn split in two ethenes or form 1-butene by 1,3-H shift. Again, the substantial barrier seen in Figure 7 is a reason to discard the pathway D_1 , too, as a significant contribution to ethene formation. Pathway D_2 in Figure 8 shows the direct formation of cyclopropane in a single step via $^3I_{1d}$. Reaction D_3 illustrates the trimethylene formation in Figure 9. Both pathways D_2 and D_3 have very high barriers as well. Thus, a reaction via $^3I_{1d}$ which yields C_3 fragments seems very unlikely.

Alternatively to the asymmetric bond breaking, symmetric bond breaking can occur. Potential curves for pathway A in Figure 10 shows the concerted fragmentation of TMSO in three fragments. A very small barrier on the S_1 (A'') potential surface has to be overcome, and adiabatic

(23) Hoffmann, R.; Swaminathan, S.; Odell, B. G.; Gleiter, R. *J. Am. Chem. Soc.* 1970, 92, 7091.

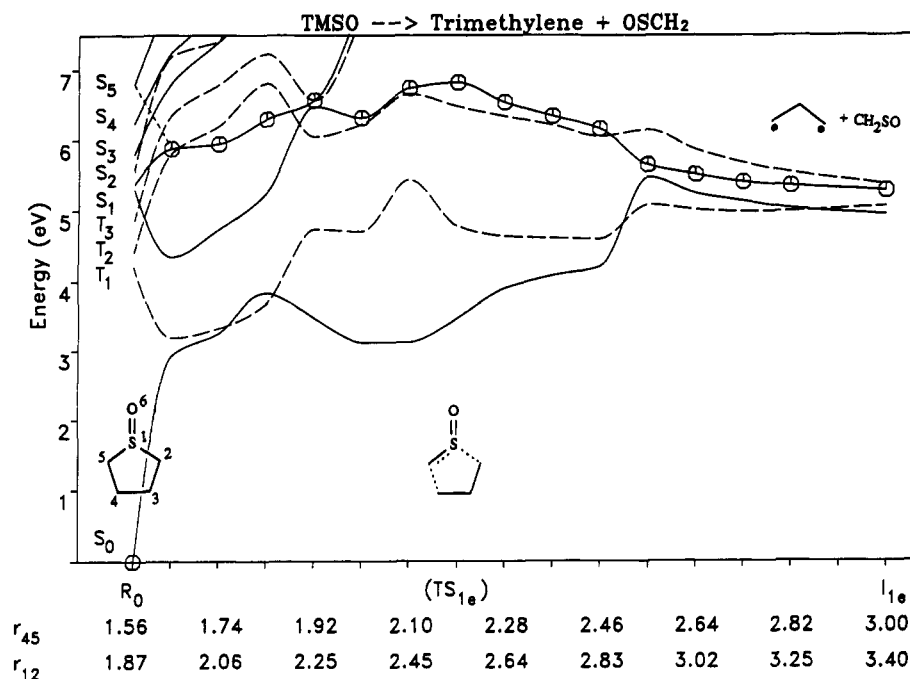


Figure 12. Potential curves for formation of trimethylene and excited CH₂SO via R₅ (A') (E); points of optimized geometry in circles.

relaxation can occur. Eventually, intersystem crossing to the triplet ground state is feasible due to the closeness of the singlet and triplet surfaces. It appears that this pathway is the main source of ethene production. P_{1α} contains the two ethenes in a singlet ground state and SO in an excited singlet state as it is predicted for an adiabatic singlet reaction by experiment.⁸ Such concerted bond-breaking reactions were already observed by experiment.^{24,25} This kind of reaction is also a matter of debate in the TMS treatment.¹⁰ Pathway B in Figure 11 shows a concerted double C-S bond rupture which yields tetramethylene and SO in a single step. After vertical excitation from the ground state to R₅ (A'') and quick IC to R₂ (A') it is easy to reach the diradical D_{1b} via adiabatic relaxation. The situation here is quite complicated since a quintet state is involved. From D_{1b} either cyclobutane, two ethenes, or 1-butene can be formed. Again an excited singlet SO is obtained. Finally, pathway E in Figure 12 illustrates the simultaneous α - and β -cleavage of TMSO. After excitation to R₅ (A'') the molecule undergoes quick IC to R₂ because of avoided crossing. The reaction coordinates are the bond lengths r_{45} and r_{12} . At $r_{45} = 1.92$ Å and $r_{12} = 2.25$ Å IC to S₁ occurs. At this point, either relaxation back to the Franck-Condon zone is possible or

photoreaction to I_{1d} after a barrier of 6.82 eV has been overcome. High pressure and low excitation energy would result in relaxation to ground-state geometry. This leads mainly to reaction pathways A and B. Thus, low pressure and high excitation energy would increase the C₃ yield. This pressure and excitation wavelength dependence of the C₃ products was essentially found by Salomon and Dorer in their experiments.⁸

4. Conclusion

From the study of TMSO photoreaction processes, a feasible sequence for the formation of the main product ethene could be established. The preferred pathway is A via direct fragmentation into two ethene and SO. The next likely pathway is B which involves the cis form of tetramethylene and should yield cyclobutane, 1-butene, and ethene. The high vibrational energy will convert cyclobutane to ethene. The formation of C₃ products could be explained by a simultaneous α - and β -cleavage. The formation of other products via triplet reactions is much less likely.

Acknowledgment. The calculations were performed on the CYBER 180/995 and Siemens S400/40 at Universität Hannover. We thank Deutsche Forschungsgemeinschaft and Fonds der Chemischen Industrie for partial support of this work. H.-P.S. thanks Prof. M. C. Zerner for his hospitality and DAAD for a research fellowship.

(24) Kim, H. L.; Satyapal, S.; Brewer, P.; Bersohn, R. *J. Chem. Phys.* **1989**, *91*, 1047.

(25) Felder, P.; Wannemacher, E. A. J.; Wiedmer, I.; Huber, J. R. *J. Am. Chem. Soc.* **1992**, *96*, 4470.